

MAGNETIC SUSCEPTIBILITY AND ANISOTROPY OF MAGNETIC SUSCEPTIBILITY: SUCCESSFUL TOOL FOR THE DETECTION OF MICROSHEAR IN SLOPE STABILITY STUDIES

Fátima Martín-Hernández^{1,2,3}, Manuel Arlandi⁴, David Lugo⁵

¹ Dep. FTAAI, Fac. CC. Físicas, Universidad Complutense de Madrid, 28040 Madrid, Spain.

² Instituto de Geociencias, IGEO (UCM, CSIC), Fac. CC. Físicas, Av. Complutense s/n, 28040 Madrid, Spain.

³ Instituto Magnetismo Aplicado (IMA) (UCM-ADIF-CSIC), Vía de Servicio A-6, 900, 28232 Las Rozas, Spain.

⁴ Túneles y Geomecánica, S.L., c/ Alfonso Gómez, 17-19, 3ª planta, Ofic. 11, 28037 Madrid, Spain

⁵ Estudio Salmer, S.L., c/Torres, 33 41002 Seville, Spain.

Abstract

Magnetic properties have been used already for decades in detection and quantification of deformation along large geological shear zones. Now, the same analysis, including Anisotropy of Magnetic Susceptibility (AMS) and total magnetic susceptibility has been applied in seven geotechnical cores. The aim is seeking for enhancements in the orientation of particles and content of magnetic minerals in strongly deformed zones. In particular, the technique has been proven to detect micro-shear zones that might develop slope instability. The presence or horizons with high value of the degree of anisotropy, increase of the total susceptibility and oblate (or flattened) ellipsoids of the magnetic anisotropy in cores dominated by clay and marly-clays is indicative of micro-deformations. This has been confirmed by further rock magnetic analysis showing that at those horizons also coercivity decreases and magnetic concentration increases.

Introduction

Magnetic susceptibility in rocks and sediments

Magnetic susceptibility is the relationship between an applied field and the magnetization in a material (e.g., Cullity, 1972). Magnetic susceptibility can also be

used as classification criteria since materials have different values depending on their nature (e.g., Dunlop and Özdemir, 1997 and references therein). Diamagnetic materials are those with a negative relationship between applied field and magnetization that disappears as soon as the magnetic field is removed. They exhibit a negative magnetic susceptibility. In nature, quartz and calcite are the most common diamagnetic materials. Paramagnetic minerals are more common in nature. Most minerals exhibit a paramagnetic behaviour. Their magnetic susceptibility is positive and they also lose magnetization when the applied field is removed. Most silicates, clays and many carbonates like siderite are paramagnetic. The third category of minerals is that of the ferromagnetic phases (*sensu lato*), those with a magnetic moment in the absence of a magnetic field. Magnetite, hematite or pyrrhotite are (using the broadest definition of the term) ferromagnetic. The relationship between applied field and magnetization is not a linear and simple function but they exhibit what is called a magnetic hysteresis, a non-linear relationship. Also important mentioning that the magnetic susceptibility is positive but several orders of magnitude higher than that in paramagnetic minerals.

Mathematically the magnetic susceptibility can be written as:

$$M = kH \quad [1]$$

where M (in A/m in the SI) is the magnetization, H the applied field (in A/m in the SI) and k is the magnetic susceptibility (dimensionless in the SI).

When measuring natural samples, magnetic susceptibility is the weighted mean of all minerals present in the sample. However, as a rule of thumb, a high

concentration of ferromagnetic minerals will mask all other contributions giving rise to susceptibility values in the order to 10^{-3} SI.

In clays and clay sediments, magnetic susceptibility is usually carried by most of the paramagnetic minerals that conform the lithology with susceptibility values in the order to 10^{-4} SI (for a review Mullins, 1977). However, those values can be modified additionally by deformation, strain, hydrothermal activity and in particular by shear strain. Large shear zones are known to be areas with a significant increase in magnetic susceptibility due to the generation of additional ferromagnetic minerals during shear associated with the slope instability (Borradaile and Henry, 1997; Ferré et al., 2014; Tarling and Hrouda, 1993). Summarizing, large variations occur only due to changes in the lithology (Figure 1a), increments in the concentration of magnetic mineral in one stratus due to microshear (Figure 1b), or other types of physic-chemical alteration (Figure 1c).

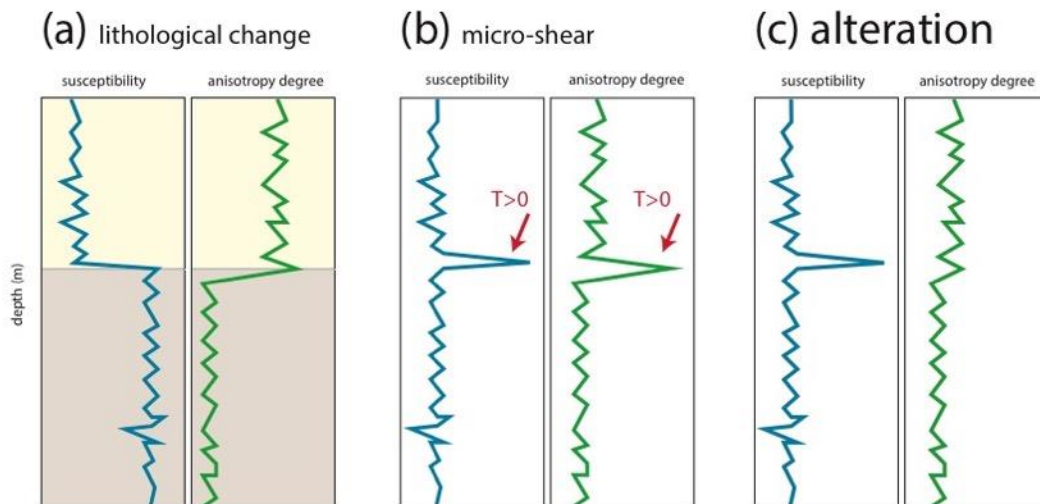


Figure 1: Schematic depiction of the variations of magnetic susceptibility and degree of anisotropy along a geotechnical core for three typical situations. A) lithological change, b) horizon with a localized microshear and c) location of one altered level.

Anisotropy of Magnetic Susceptibility (AMS)

Anisotropy of Magnetic Susceptibility (AMS) is the spatial variation of the magnetization vs. applied field depending on the orientation. If the susceptibility is not isotropic, then Eq [1] should be written in tensorial notation. The susceptibility is therefore a symmetric matrix:

$$\mathbf{M} = \begin{bmatrix} k_{11} & k_{12} & k_{13} \\ k_{12} & k_{22} & k_{23} \\ k_{13} & k_{23} & k_{33} \end{bmatrix} \mathbf{H} \quad [2]$$

It is commonly represented by an ellipsoid with semi-axes equal to the principal values of the susceptibility matrix with $k_3 \geq k_2 \geq k_1$ and the orientation of the eigenvectors. The three principal values of the AMS ellipsoid are usually summarized in two parameters, i) degree of anisotropy or eccentricity of the ellipsoid (P_j) and ii) shape of the ellipsoid (T) (Tarling and Hrouda, 1993). The degree of anisotropy is a proxy for the degree of alignment of minerals reaching the maximum value when all minerals are perfectly aligned and behave as one single crystal. This holds true for paramagnetic and diamagnetic minerals. If also ferromagnetic particles are present, P_j increases dramatically since the intrinsic value of anisotropy of those particles is higher. The shape of the AMS ellipsoid can vary from oblate ($0 \leq T \leq 1$) to prolate ($-1 \leq T \leq 0$) and it can also be used as an indicator of alignment when the composition and single crystal properties of the components is known (Martín-Hernández et al., 2004). In the particular case of clays and marly clays, composed basically by phyllosilicates, values of T are commonly oblate. Numerically, P_j and T are defined by:

$$\begin{aligned}
h_1 &= \log(k_1); h_2 = \log(k_2); h_3 = \log(k_3); h_m = \left(\frac{h_1 + h_2 + h_3}{3} \right) \\
P_j &= \exp\left(\sqrt{2\left((h_1 - h_m)^2 + (h_2 - h_m)^2 + (h_3 - h_m)^2 \right)} \right) \quad [3] \\
T &= \frac{2h_2 - h_1 - h_3}{h_1 - h_3}
\end{aligned}$$

In clays and marly clays, magnetic anisotropy is usually very low, increasing the value with deformation (Cifelli et al., 2009; Cifelli et al., 2004). The technique has been proven to be extremely sensitive to incipient deformation in these lithologies (Caricchi et al., 2016; Soto et al., 2009). Common values might range between 1.03 (Cifelli et al., 2004) and 1.35, which is the single crystal value for pure biotite (Martin-Hernandez and Hirt, 2003). Variations in depth are commonly associated to changes in lithology (Figure 1a).

In shear zones the particles orient in the direction of shear increasing the degree of anisotropy (Mamtani and Sengupta, 2009). Also, the accumulation of stress and subsequent deformation induces the formation of newly ferromagnetic minerals (mainly iron oxides such as magnetite) that increase the total susceptibility at the location of the deformation band (Borradaile and Jackson, 2004) (Figure 1b).

The increase of degree of anisotropy with deformation is well documented from the sedimentary fabric to the metamorphic slates and shales, with the results of an increment of the degree of anisotropy (Parés, 2015). In the absence of deformation, clays have a poor anisotropy with the phyllosilicates laying along the bedding plane due to depositional mechanisms (Figure 2a). The direction of shear behaves as a plane in which mainly phyllosilicates but also ferromagnetic grains orient, given rise to the observed enhancement of degree of anisotropy (Figure 2b).

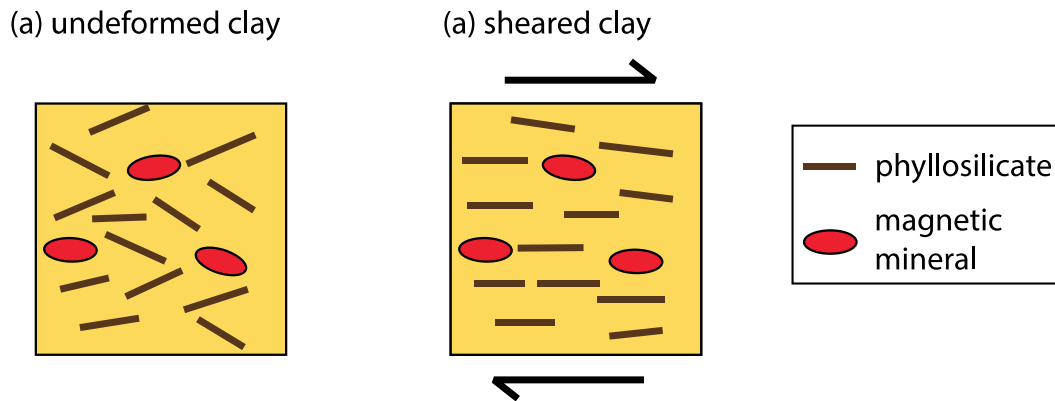


Figure 2: Conceptual sketch of the enhancement of orientation in a clay rich sediment due to a shear zone. The original orientation of minerals is poor and related to deposition a) and it increases the orientation in the direction of shear b).

These, together with an enhancement of the total susceptibility due to the formation of new iron oxides during deformation forms a tool of three parameters that conforms a proxy indicative of micro-shear zones.

Methodology

Sampling and field-work

Seven geotechnical cores have been extracted in the area under study following a strict protocol that excludes the use of metallic tools and cools extremely well the drill. Cores have been labelled as GS1 to GS7. Lithologically speaking, cores are characterized by four levels identify as marly clays with different clay content including one anthropogenic level in the upper part (from 0-3 meters). A general description can be found in Table I.

name	Thickness (m)	description
GL1-Geotechnical level 1	0-1 m	Anthropic sediment and infilling
GL2-Geotechnical level 2	6-15 m	Brown marly clay with different contents of fine sands
GL3-Geotechnical level 3	2-6 m	Transition level. Hard brown marly clays to clays
GL4-Geotechnical level 4	Basal level at the bottom of the cores	Miocene substratum, hard grey marly clay

Table I: General description of the lithology found in the seven geotechnical cores.

In the extraction process, no metallic tools have been used in order to prevent alteration of the magnetization and magnetic properties. After the extraction, the material has been sub-samples using plastic boxes as those used in paleomagnetic studies granting no magnetic impurities that alter the results. All the plastic boxes have to be sealed in case of including a little hole in the bottom of the box in order to keep the moist level in similar conditions as those in situ (Figure 3a). The sediments have been extracted from the core, placing the plastic boxes and pressing gently, after removing all the material exciding the box with a plastic tool (Figure 3b), boxes have been cover with a their lid and labelled (Figure 3c). A total of 345 samples distributed along the seven cores have been samples at an average distance of 50 cm between samples in the core.



Figure 3: Core sediments sampling and extraction protocol. a) extraction of the sediments from the geotechnical core, b) selection of the material and c) storing and labelling of the sub-samples.

Magnetic susceptibility

Magnetic susceptibility has been measured in a KLY-4S susceptibility bridge manufactured by AGICO with a sensitivity of $2 \cdot 10^{-8}$ SI at the operating field of 300 A/m and 850 Hz of Frequency. Each specimen has been measured in three

perpendicular positions and the average value has been used as the mean susceptibility. Measurements have been carried out in the 345 samples inspecting increments of magnetic susceptibility associated with deformation.

Anisotropy of Magnetic Susceptibility (AMS)

AMS has been measured in an AGICO KLY-4S susceptibility bridge provided with a rotating head for anisotropy measurements. Each samples has been measured in three perpendicular planes in order to determine the best magnetic susceptibility tensor fitted from the data by a least square procedure (Jelinek, 1973). Due to the weak anisotropy of undeformed sediments, an statistical anisotropy F-test (Fisher statistical test) has been carried out (Borradaile, 2003). The measured anisotropy ellipsoid is compared with the corresponding isotropic tensor. The null hypothesis (isotropic tensor) is neglected when then F-value is compared with a Fisher distribution. If the obtained value is larger than that of the Fisher distribution (in the case under study is $F=4.25$) then the samples is anisotropic (Borradaile, 2003; Jelinek, 1978). After confirming the magnetic anisotropy of the 345 samples, the AMS ellipsoid, principal values and their orientation, degree of anisotropy and shape of the ellipsoid has been computed following Eq. [3] looking for increments in anisotropy due to deformation.

Magnetic hysteresis

Magnetic hysteresis loops were measured using a coercivity spectrometer (Jasonov et al., 1998) with a maximum applied field of 0.5 T including the initial magnetization curve in all samples of one geotechnical core and selected samples

from the other six. The aim is characterizing possible variations in the ferromagnetic particles in the deformed area.

Derived from the hysteresis curves, the saturation magnetization (M_s), saturation magnetization of remanence (M_{rs}) and coercitive force (H_c) have been derived. Previously, all samples have been corrected by the magnetization of the paramagnetic contribution, which has been computed as the linear term after the saturation of the ferromagnetic phases (Dunlop and Özdemir, 1997).

Isothermal Remanent Magnetization (IRM) and coercivity spectral analysis

Acquisition of Isothermal REmanente Magnetization curves (IRM) has been measured in all samples up to 0.5 T using also coercivity spectrometer (Jasonov et al., 1998). After saturation of magnetization, subsequent back field CD demagnetization of isothermal remanence has been measured, allowing the characterization of the coercivity of remanence (H_{cr}). Measurements have been carried out in the samples where magnetic hysteresis has been determined.

The IRM - acquisition curves were modeled by a series of log-normal distributions of the IRM gradient in order to infer the coercivity distribution associated to magnetic fractions. The mathematical fitting has been modeled by the method outlined by Kruiver et al. (2001) and the associated software. This provides an excellent description of the distribution of magnetic particles, their coercivity and concentration. The mean value of the main distribution is good explanation of the “magnetic hardness”.

Results

Magnetic susceptibility and magnetic anisotropy profiles

The results of the seven geotechnical cores have been analysed in the present work. The anisotropy of magnetic susceptibility and total susceptibility have been measured in discrete samples extracted every 50 cm in order to detect the presence of incipient shear zones that might develop instability in the corresponding slope.

The study has focused the attention on strong variations of magnetic anisotropy degree with values larger than 1.10 that would represent a 10% of anisotropy and values of the total magnetic susceptibility larger than the average of the total core $\pm 2\sigma$, being σ the standard deviation of the mean value. The detection of anomalous points must coincide also with samples with oblate AMS ellipsoids. Results of the seven analysed cores can be found in Figure 4 to Figure 10 together with the geological description of the lithology.

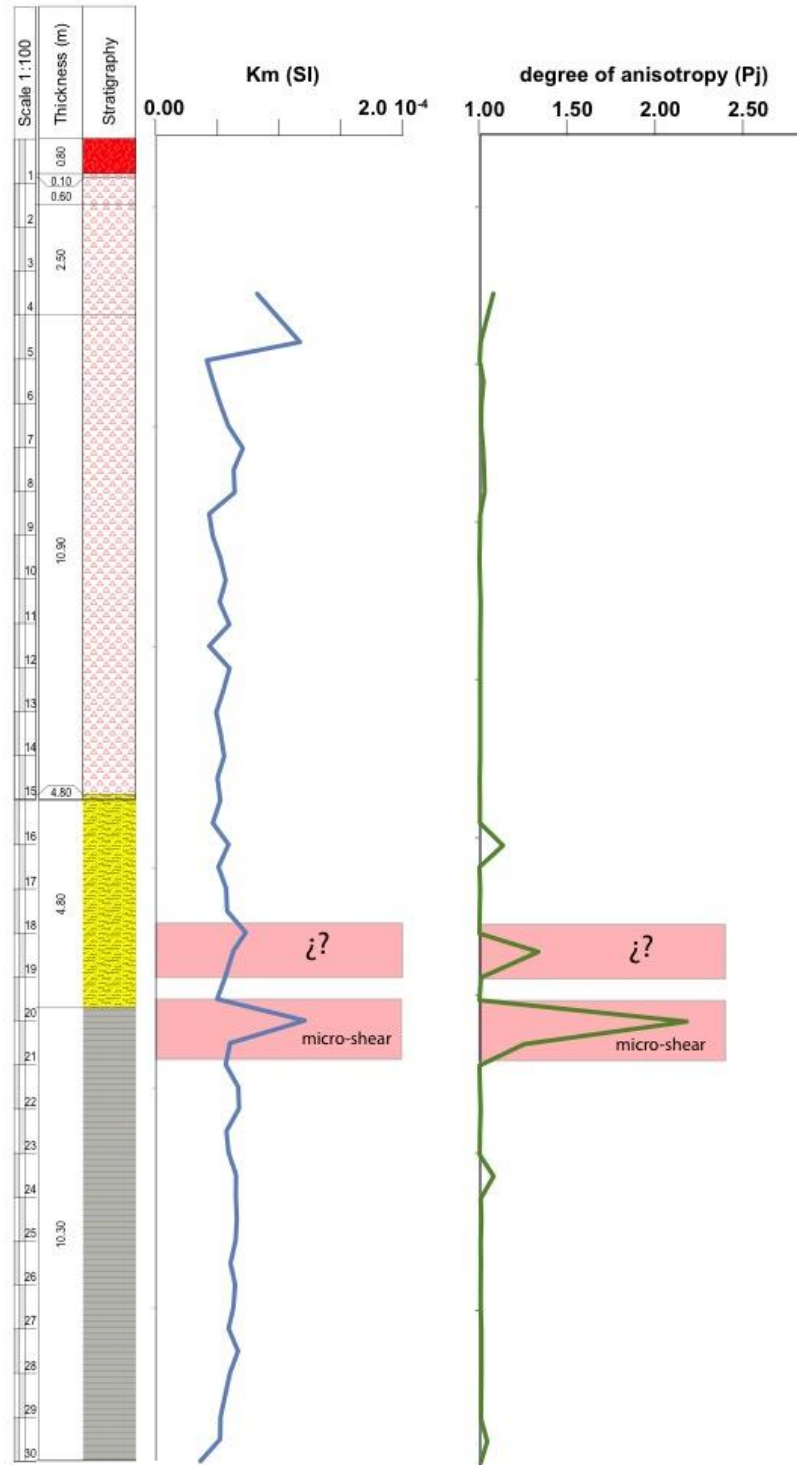


Figure 4: Lithological profile, magnetic susceptibility along the geotechnical core and degree of anisotropy measured in core SG-1.

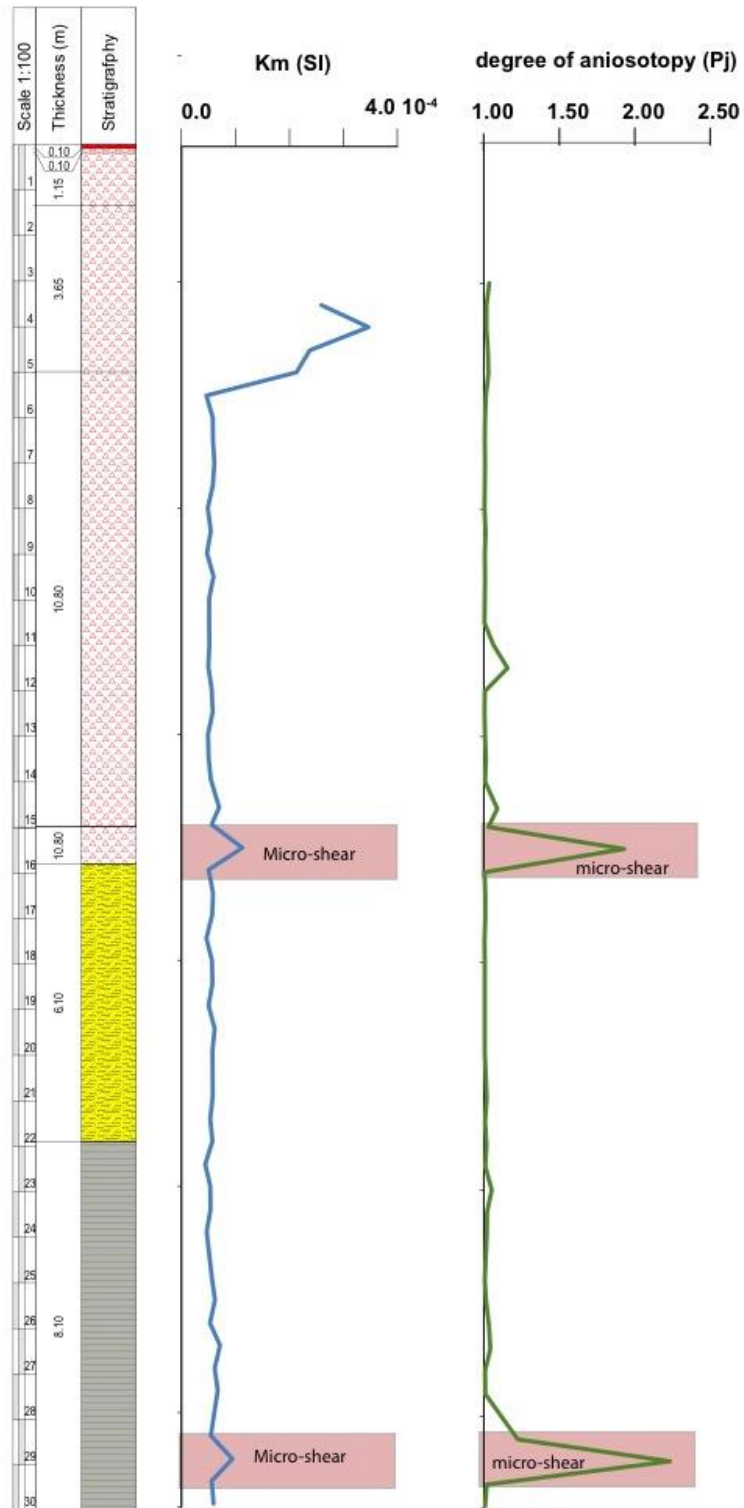


Figure 5: Lithological profile, magnetic susceptibility along the geotechnical core and degree of anisotropy measured in core SG-2.

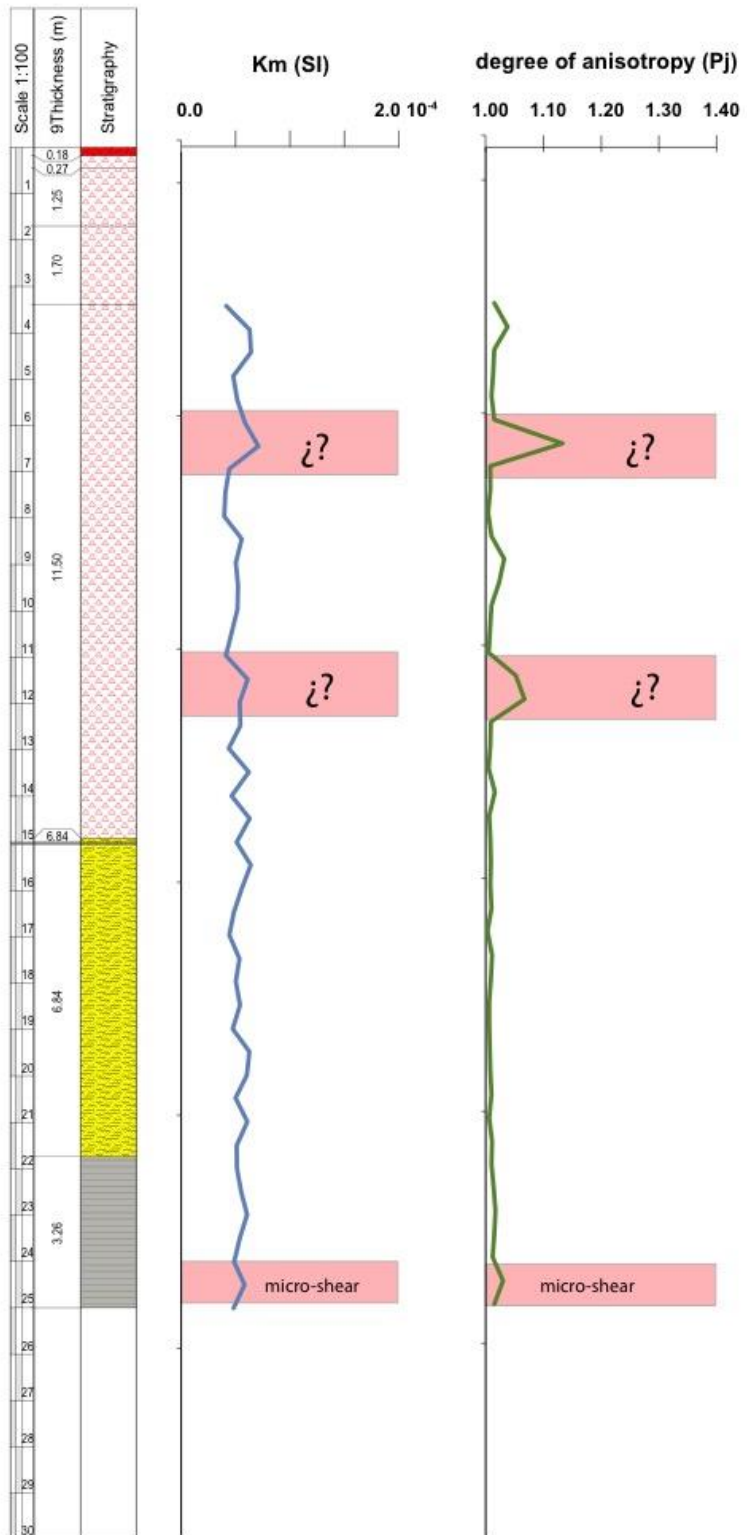


Figure 6: Lithological profile, magnetic susceptibility along the geotechnical core and degree of anisotropy measured in core SG-3.

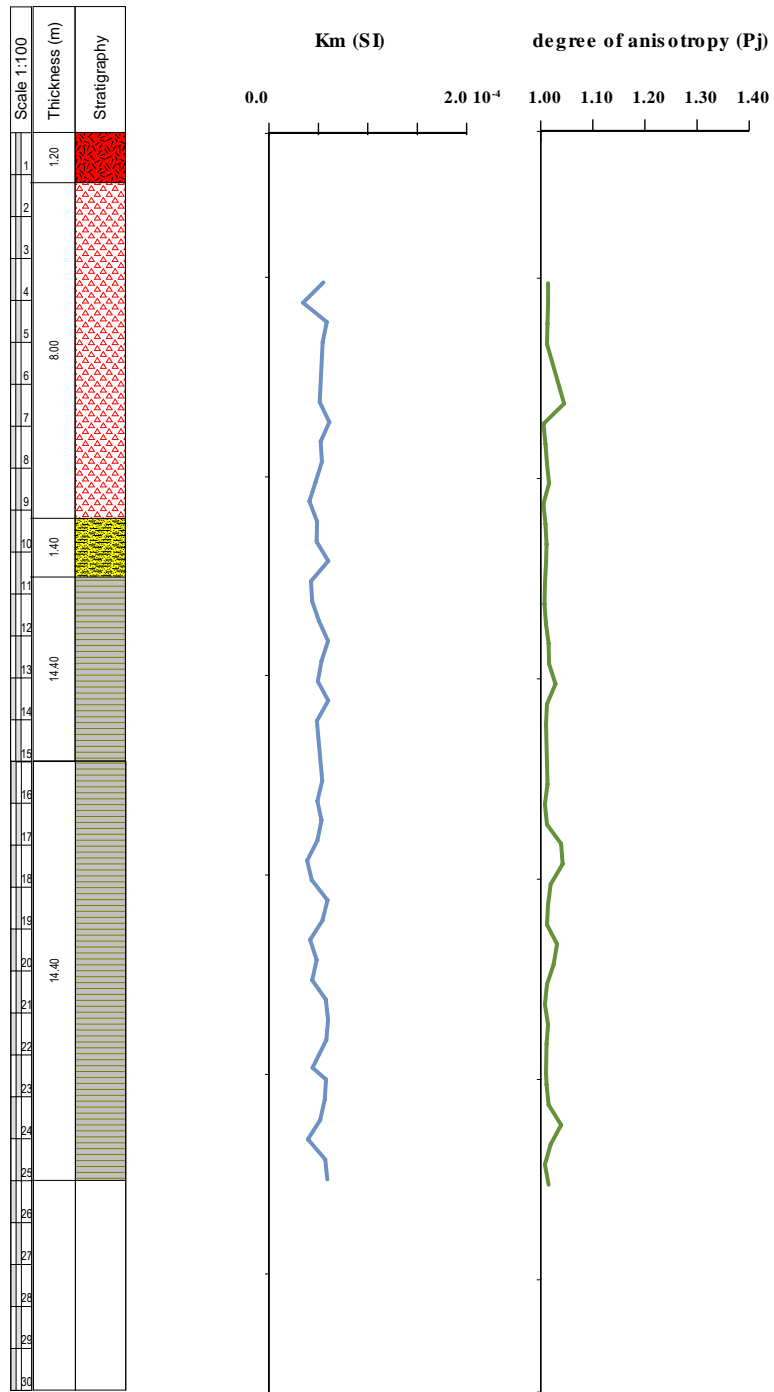


Figure 7: Lithological profile, magnetic susceptibility along the geotechnical core and degree of anisotropy measured in core SG-4.

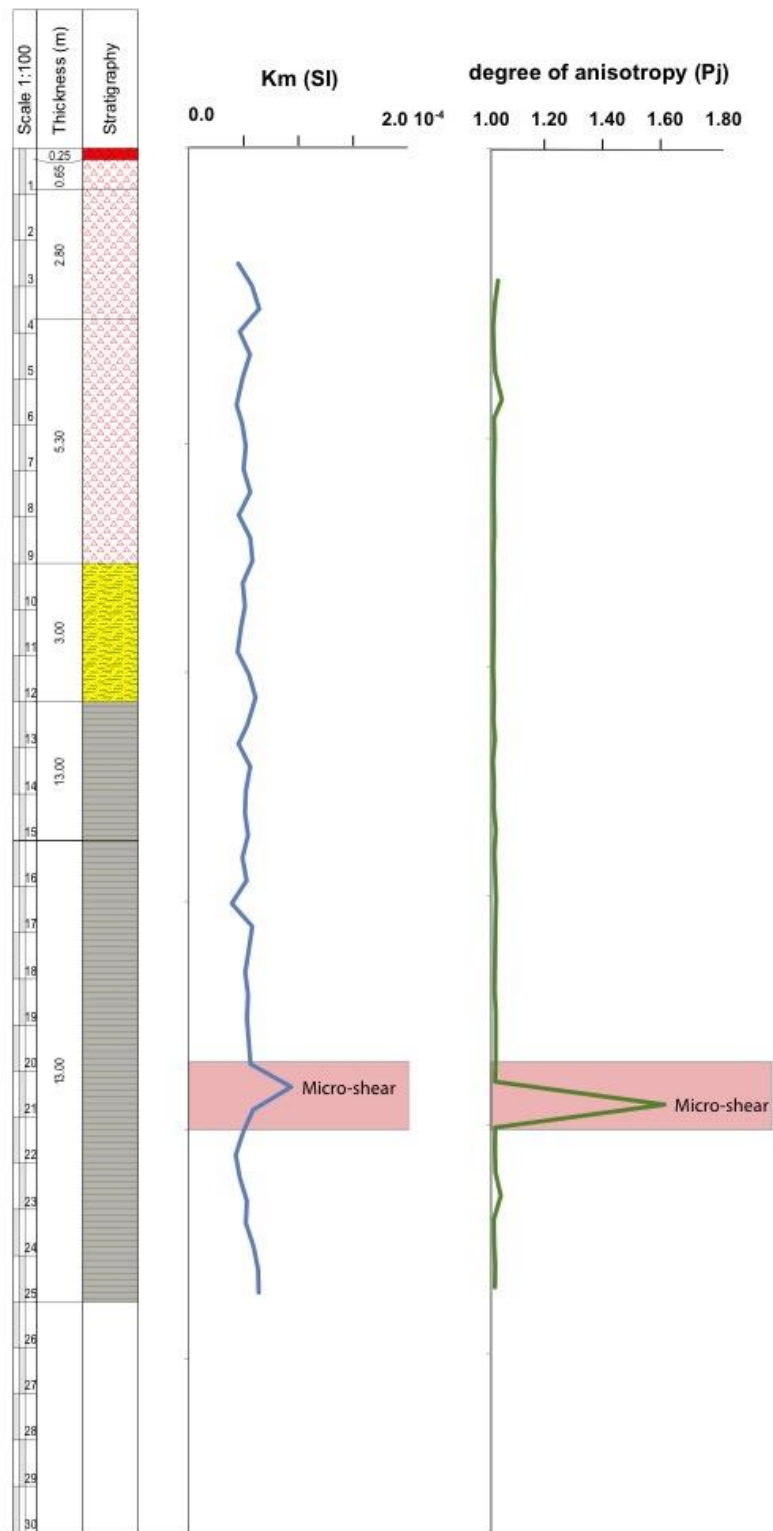


Figure 8: Lithological profile, magnetic susceptibility along the geotechnical core and degree of anisotropy measured in core SG-5.

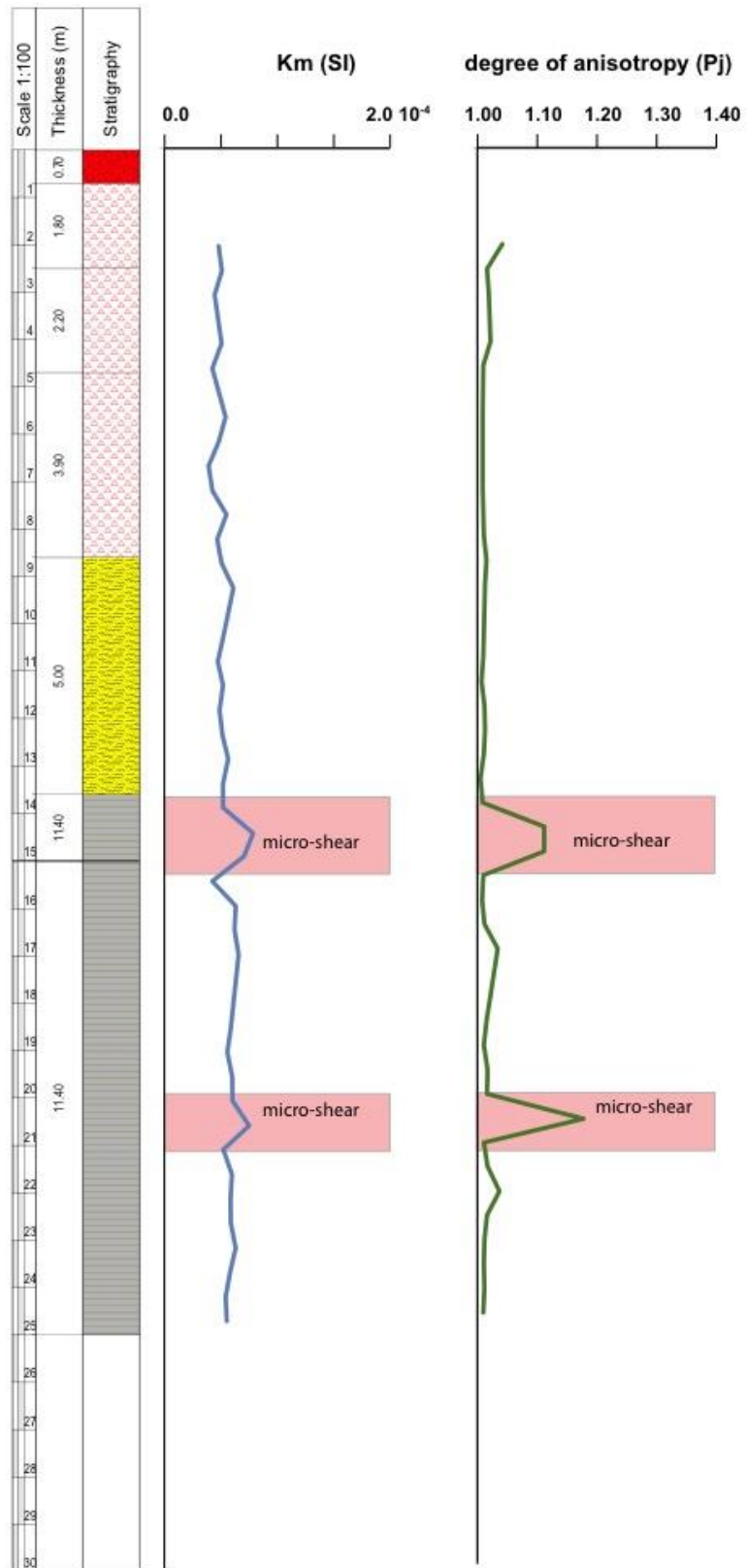


Figure 9: Lithological profile, magnetic susceptibility along the geotechnical core and degree of anisotropy measured in core SG-6.

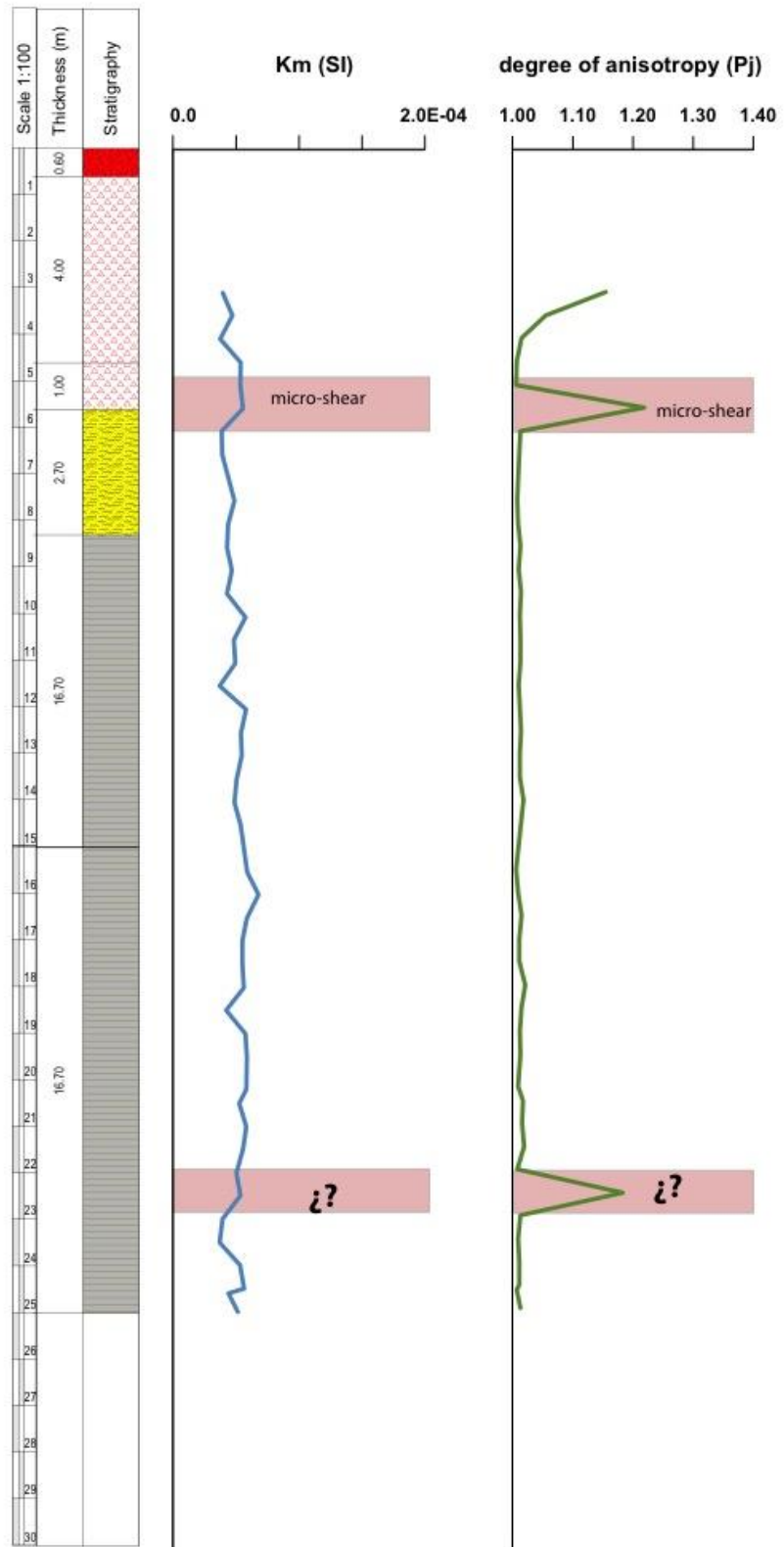


Figure 10: Lithological profile, magnetic susceptibility along the geotechnical core and degree of anisotropy measured in core SG-7.

Results of magnetic hysteresis at the anomaly and adjacent points

In order to add more information about the magnetic enhancement process occurring in the microshear zone of geotechnical cores, intensive rock magnetic analysis have been carried out at the anomalous points highlighted in in Figure 4 to Figure 10 and samples immediately above and below. This includes magnetic hysteresis up to 500 mT. This experiment reveals information about concentration of ferromagnetic minerals (given by the M_s parameter) and hardness of the ferromagnetic minerals (given by H_c).

Figure 11a illustrates the typical behaviour of one sample located at the level of one identified microshear zone with high values of magnetic susceptibility and high values of the magnetic anisotropy. Magnetic hysteresis is noisy and only after the correction for the paramagnetic susceptibility of the sediments the magnetic hysteresis loop is seen. This confirms the low concentration of ferromagnetic minerals.

Figure 11b illustrates the values of M_s , magnetic saturation as a function of depth for samples in the core SG-1. Sample in red represents the data from the adjacent figure showing that samples with an increase of magnetic susceptibility and an increase of magnetic anisotropy also experiment high values of the magnetic saturation.

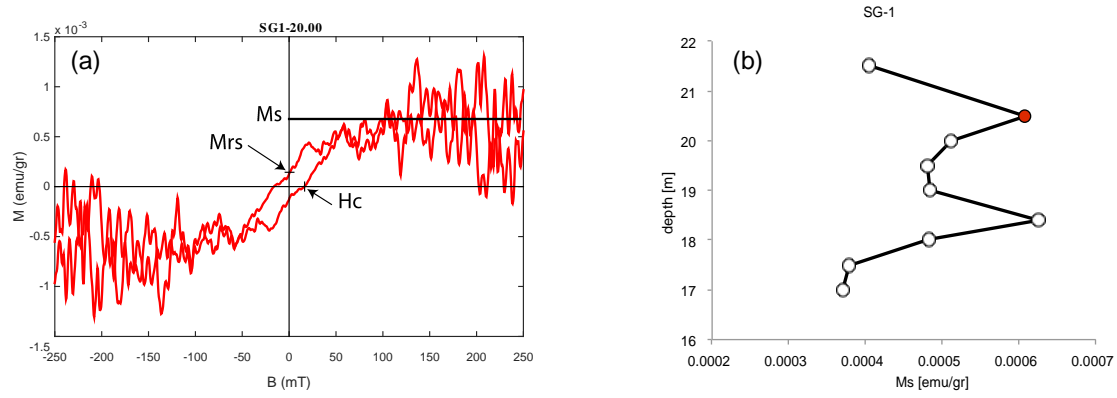


Figure 11: a) Magnetic hysteresis of sample SG1-20, located at one of the points identified as a micro-shear zone and b) profile of saturation magnetization (M_s) along the SG1 core. Red point indicate sample shown in the corresponding left panel of the figure.

All data derived from hysteresis are summarized in Table II. All detected points with high values of susceptibility and degree of anisotropy have an increase of M_s with the exception of samples from core SG-6.

Table II: Table summarizing all the magnetic parameters derived from hysteresis loops in samples highlighted as possible levels with microshear and samples immediately above and below. Samples of interest have been labelled with a *.

name	Depth (m)	M_s (emu/gr)	M_r (emu/gr)	H_c (mT)	H_{cr} (mT)
SG1-1700	17	$3.70 \cdot 10^{-4}$	$9.30 \cdot 10^{-5}$	4.07	34.09
SG1-1750	17.5	$3.79 \cdot 10^{-4}$	$7.10 \cdot 10^{-5}$	4.09	34.09
SG1-1800B	18	$4.83 \cdot 10^{-4}$	$1.36 \cdot 10^{-4}$	2.94	34.13
SG1-1840B	18.4*	$6.26 \cdot 10^{-4}$	$1.48 \cdot 10^{-4}$	5.07	32.84
SG1-1900B	19	$4.84 \cdot 10^{-4}$	$1.34 \cdot 10^{-4}$	4.19	31.16
SG1-1950B	19.5	$4.81 \cdot 10^{-4}$	$1.11 \cdot 10^{-4}$	3.67	30.7
SG1-2000B	20*	$5.12 \cdot 10^{-4}$	$1.43 \cdot 10^{-4}$	4.54	33.28
SG1-2050B	20.5	$6.08 \cdot 10^{-4}$	$1.87 \cdot 10^{-4}$	14.39	33.86
SG1-2150	21.5	$4.04 \cdot 10^{-4}$	$9.60 \cdot 10^{-5}$	8.04	33.97
SG2-1400	14	$4.40 \cdot 10^{-4}$	$1.11 \cdot 10^{-4}$	9.77	45.17
SG2-1460	14.6	$6.36 \cdot 10^{-4}$	$2.62 \cdot 10^{-4}$	5.95	43.76
SG2-1500B	15	$1.10 \cdot 10^{-3}$	$2.27 \cdot 10^{-4}$	5.6	24.59
SG2-1550B	15.5*	$1.25 \cdot 10^{-3}$	$1.29 \cdot 10^{-4}$	4.71	30.83
SG2-1600B	16	$3.92 \cdot 10^{-4}$	$1.25 \cdot 10^{-4}$	4.14	26.51
SG2-1650	16.5	$4.26 \cdot 10^{-4}$	$1.22 \cdot 10^{-4}$	3.82	59.42
SG2-2700	27	$4.36 \cdot 10^{-4}$	$9.40 \cdot 10^{-5}$	4.72	44.41
SG2-2750	27.5	$4.32 \cdot 10^{-4}$	$1.10 \cdot 10^{-4}$	5.16	34.1
SG2-2850B	28.5	$4.59 \cdot 10^{-4}$	$1.30 \cdot 10^{-4}$	10.74	30.26
SG2-2900B	29*	$6.50 \cdot 10^{-4}$	$1.30 \cdot 10^{-4}$	2.13	30.78
SG2-2950B	29.5	$4.32 \cdot 10^{-4}$	$1.30 \cdot 10^{-4}$	4.11	31.64
SG3-2300	23	$3.81 \cdot 10^{-4}$	$1.20 \cdot 10^{-4}$	7.01	32.95
SG3-2350B	23.5	$8.39 \cdot 10^{-4}$	$2.64 \cdot 10^{-4}$	13.58	40.47
SG3-2400B	24	$4.62 \cdot 10^{-4}$	$1.12 \cdot 10^{-4}$	12.47	32.65
SG3-2450B	24.5*	$1.07 \cdot 10^{-3}$	$1.94 \cdot 10^{-4}$	6.42	28.24
SG3-2500B	25	$7.66 \cdot 10^{-4}$	$1.62 \cdot 10^{-4}$	8.9	29.46
SG5-1900B	19	$1.32 \cdot 10^{-3}$	$2.97 \cdot 10^{-4}$	10	37.93
SG5-2000B	20	$1.02 \cdot 10^{-3}$	$2.36 \cdot 10^{-4}$	12.4	42.48
SG5-2050B	20.5	$9.62 \cdot 10^{-3}$	$9.06 \cdot 10^{-4}$	6.95	27.86
SG5-2100B	21*	$6.91 \cdot 10^{-4}$	$1.56 \cdot 10^{-4}$	5.15	34.91
SG5-2150B	21.5	$7.35 \cdot 10^{-4}$	$1.58 \cdot 10^{-4}$	6.06	34.21

SG5-2200B	22	3.03 10 ⁻³	4.56 10 ⁻⁴	10.31	25.14
SG5-2250B	22.5	2.19 10 ⁻³	2.72 10 ⁻⁴	11.65	42.01
SG6-1250B	12.5	2.50 10 ⁻³	2.64 10 ⁻⁴	12.08	43.86
SG6-1300B	13	1.73 10 ⁻³	2.37 10 ⁻⁴	10.03	42.35
SG6-1350B	13.5	1.39 10 ⁻³	3.04 10 ⁻⁴	6.75	27.24
SG6-1400B	14*	5.19 10 ⁻⁴	8.10 10 ⁻⁵	14.22	34.3
SG6-1450B	14.5	5.07 10 ⁻⁴	8.30 10 ⁻⁵	4.99	34.26
SG6-1500B	15	2.06 10 ⁻³	2.63 10 ⁻⁴	9.01	44.56
SG6-1550	15.5	2.67 10 ⁻³	2.20 10 ⁻⁴	8.53	41.2
SG6-1850	18.5	2.11 10 ⁻³	1.95 10 ⁻⁴	9.3	43.55
SG6-1900R	19	2.02 10 ⁻³	2.09 10 ⁻⁴	8.97	36.7
SG6-2000B	20*	9.55 10 ⁻⁴	1.41 10 ⁻⁴	4.03	32.15
SG6-2050B	20.5	1.84 10 ⁻³	1.95 10 ⁻⁴	3.85	30.35
SG6-2100	21	2.72 10 ⁻³	2.42 10 ⁻⁴	9.04	42.33
SG6-2150	21.5	1.93 10 ⁻³	2.56 10 ⁻⁴	6.49	42.12
SG7-0400	4	1.70 10 ⁻³	1.71 10 ⁻⁴	5.09	32.91
SG7-0450	4.5	9.29 10 ⁻⁴	1.49 10 ⁻⁴	6.4	36.31
SG7-0500	5*	6.59 10 ⁻⁴	1.24 10 ⁻⁴	3.94	39.57
SG7-0550	5.5	7.67 10 ⁻⁴	1.64 10 ⁻⁴	4.81	33.51
SG7-0600B	6	1.32 10 ⁻³	1.43 10 ⁻⁴	4.89	34.75
SG7-0650	6.5	7.14 10 ⁻⁴	8.70 10 ⁻⁵	4.69	35.43
SG7-2100	21	6.52 10 ⁻⁴	8.30 10 ⁻⁵	3.23	34.57
SG7-2150	21.5	6.25 10 ⁻⁴	1.00 10 ⁻⁴	2.99	33.21
SG7-2200B	22	9.61 10 ⁻⁴	1.29 10 ⁻⁴	6.57	31.65
SG7-2250B	22.5*	8.67 10 ⁻⁴	1.83 10 ⁻⁴	6.75	30.96
SG7-2300B	23	4.83 10 ⁻⁴	1.34 10 ⁻⁴	7.44	32.59
SG7-2350	23.5	6.71 10 ⁻⁴	6.60 10 ⁻⁵	4.09	33.85
SG7-2400	24	6.30 10 ⁻⁴	5.60 10 ⁻⁵	0.6	37.12

Results from Isothermal Remanent Magnetization (IRM) and coercivity spectral analysis

IRM acquisition curves show the capacity to retain magnetization of the ferromagnetic particles. Each ferromagnetic grain is able to keep a magnetization until it saturates and the field at which this happens varies depending on the type of magnetic minerals. IRM acquisition curves look very similar in all analysed samples observing no differences depending on the position of the samples. Figure 12 shows one example of this behaviour.

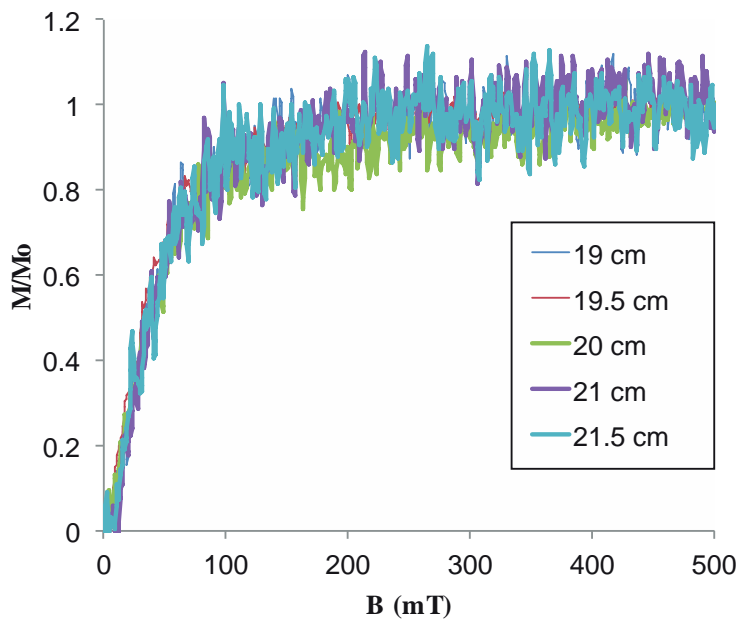


Figure 12: IRM acquisition curves for sample SG1-20 and samples immediately above and below.

A further investigation on the IRM curves reveals interesting facts. The derivative curve of those shown in Figure 12 is also an indicator of the nature of magnetic particles. It highlights the mean coercivity or hardness of the population of magnetic particles. Figure 13 exemplifies the findings. Samples where micro-shear has been detected (at depth 20 cm in the example) have the mean coercivity of the ferromagnetic fraction (given by the pick in the curve) at lower values. This behaviour has been found at all levels where magnetic susceptibility increases and degree of anisotropy too.

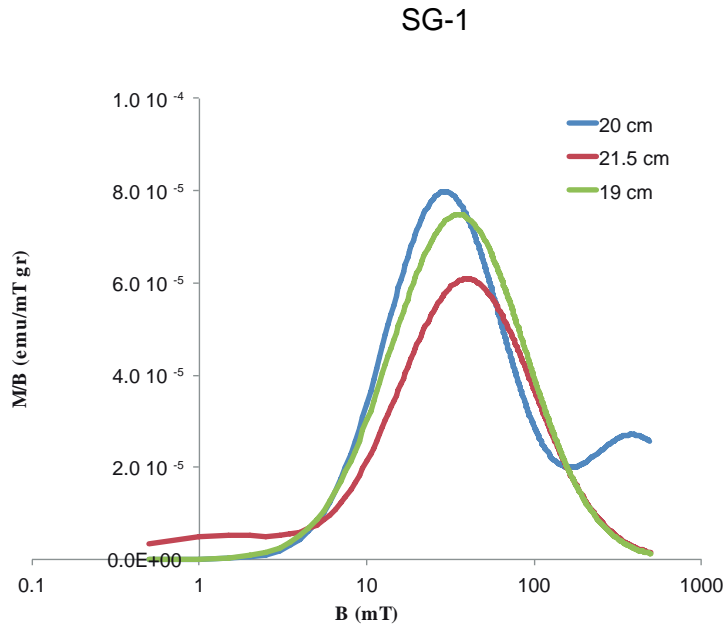


Figure 13: Coercivity spectra or first derivative of the IRM acquisition curve in three samples from core SG-1. Anomalous point at depth 20 cm and adjacent points are shown for simplicity.

Back field IRM, which is a similar experiment as previously shown in Figure 12 but with the applied field in opposite direction, allows computing the also called coercivity of remanence (H_{cr}). This parameter measures the difficulty to erase a remanence on the ferromagnetic particles. Table II summarizes the results from this experiment in most significant samples from this study. There is a tendency to decrease the coercivity of remanence nearby the points where microshears have been detected by other magnetic procedures.

Conclusions

The final result of the current study allows presenting three key points that summarize it:

- The combination of total magnetic susceptibility and anisotropy of magnetic susceptibility along the profile of geotechnical cores is a useful technique to detect micro-shear levels.

- Following the indications already developed in geological shear zones, micro-deformations develop an increase of the anisotropy degree and the total magnetic susceptibility.
- In our study, deformation is accumulated in the contact between geotechnical levels but also has been found within the lower geotechnical level, suggesting instability might be deeper than expected.
- The anomalous points are characterized by an increase in the magnetic concentration, confirmed by an increase in Ms.
- At those levels, also coercivity decreases, suggested by a lower value of Hcr and confirmed by a lower value of the pick in the coercivity spectra.

References

Borradaile, G. J. (2003), *Statistics of Earth Science Data, Space and Orientation*, 351 pp., Springer.

Borradaile, G. J., and B. Henry (1997), Tectonic applications of magnetic susceptibility and its anisotropy, *Earth-Science Reviews*, 42, 49-93.

Borradaile, G. J., and M. Jackson (2004), Anisotropy of magnetic susceptibility (AMS): magnetic petrofabrics of deformed rocks, in *Magnetic Fabric: Methods and Applications*, edited by F. Martín-Hernández, C. Lüneburg, C. Aubourg and M. Jackson, pp. 299-360, Geological Society of London, London.

Caricchi, C., F. Cifelli, C. Kissel, L. Sagnotti, and M. Mattei (2016), Distinct magnetic fabric in weakly deformed sediments from extensional basins and fold-and-thrust structures in the Northern Apennine orogenic belt (Italy), *Tectonics*, 35(2), 238-256, doi:10.1002/2015TC003940.

Cifelli, F., M. Mattei, M. Chadima, S. Lenser, and A. M. Hirt (2009), The magnetic fabric in “undeformed clays”: AMS and neutron texture analyses from the Rif Chain (Morocco), *Tectonophysics*, 466(1-2), 79-88, doi:<https://doi.org/10.1016/j.tecto.2008.08.008>.

Cifelli, F., M. Mattei, A. M. Hirt, and A. Gunter (2004), The origin of tectonic fabric in "undeformed" clays: The early stages of deformation in extensional sedimentary basins, *Geophysical Research Letters*, 31, doi:10.1029/2004GL019609.

Cullity, B. D. (1972), *Introduction to Magnetic Materials*, 666 pp., Addison-Wesley, Reading, MA.

Dunlop, D. J., and Ö. Özdemir (1997), *Rock Magnetism: Fundamentals and Frontiers*, 573 pp., Cambridge University Press, Cambridge.

Ferré, E. C., A. Gébelin, J. L. Till, C. Sassier, and K. C. Burmeister (2014), Deformation and magnetic fabrics in ductile shear zones: A review, *Tectonophysics*, 629, 179-188, doi:<http://dx.doi.org/10.1016/j.tecto.2014.04.008>.

Jasonov, P. G., D. K. Nougaliiev, B. V. Burov, and F. Heller (1998), A modernized coercivity spectrometer, *Geologica Carpathica*, 49, 224-225.

Jelinek, V. (1973), Precision A.C. bridge set for measuring magnetic susceptibility of rocks and its anisotropy, *Studia geoph. et geod.*, 17, 36-48.

Jelinek, V. (1978), Statistical processing of magnetic susceptibility measured on groups of specimens, *Stud. Geophys. Geod.*, 22, 50-62.

Kruiver, P. P., M. J. Dekkers, and D. Heslop (2001), Quantification of magnetic coercivity components by the analysis of acquisition curves of isothermal remanent magnetisation, *Earth and Planetary Science Letters*, 189(3-4), 269-276.

Mamtani, M. A., and A. Sengupta (2009), Anisotropy of magnetic susceptibility analysis of deformed kaolinite: implications for evaluating landslides, *International Journal of Earth Sciences*, 98(7), 1721-1725, doi:10.1007/s00531-008-0336-x.

Martin-Hernandez, F., and A. M. Hirt (2003), Paramagnetic anisotropy of magnetic susceptibility in biotite, muscovite and chlorite single crystals, *Tectonophysics*, 367(1-2), 13-28.

Martín-Hernández, F., C. Lüneburg, C. Aubourg, and M. Jackson (2004), *Magnetic Fabric: Methods and Applications*, 560 pp., Geological Society of London, London.

Mullins, C. E. (1977), Magnetic susceptibility of the soil and its significance in soil science – a review, *Journal of Soil Science*, 28(2), 223-246, doi:10.1111/j.1365-2389.1977.tb02232.x.

Parés, J. M. (2015), Sixty years of anisotropy of magnetic susceptibility in deformed sedimentary rocks, *Frontiers in Earth Science*, 3(4), doi:10.3389/feart.2015.00004.

Soto, R., J. C. Larrasoana, L. E. Arlegui, E. Beamud, B. Oliva-Urcia, and J. L. Simón (2009), Reliability of magnetic fabric of weakly deformed mudrocks as a palaeostress indicator in compressive settings, *Journal of Structural Geology*, 31(5), 512-522, doi:<http://dx.doi.org/10.1016/j.jsg.2009.03.006>.

Tarling, D. H., and F. Hrouda (1993), *The Magnetic Anisotropy of Rocks*, 217 pp., Chapman & Hall, London.